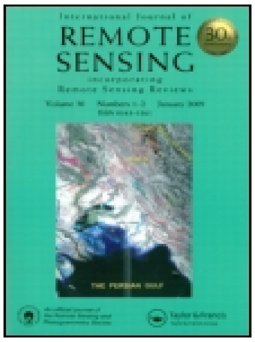

International Journal of Remote Sensing

ISSN: 0143-1161 (Print) 1366-5901 (Online) Journal homepage: https://www.tandfonline.com/loi/tres20

Estimating landscape-scale vegetation carbon stocks using airborne multi-frequency polarimetric synthetic aperture radar (SAR) in the savannahs of north Australia

J. N. Collins , L. B. Hutley , R. J. Williams , G. Boggs , D. Bell & R. Bartolo

To cite this article: J. N. Collins , L. B. Hutley , R. J. Williams , G. Boggs , D. Bell & R. Bartolo (2009) Estimating landscape-scale vegetation carbon stocks using airborne multi-frequency polarimetric synthetic aperture radar (SAR) in the savannahs of north Australia, International Journal of Remote Sensing, 30:5, 1141-1159, DOI: 10.1080/01431160802448935

To link to this article: https://doi.org/10.1080/01431160802448935

Published online: 08 Apr 2009.

International Journal of Remote Sensing
Vol. 30, No. 5, 10 March 2009, 1141–1159

Estimating landscape-scale vegetation carbon stocks using airborne multi-frequency polarimetric synthetic aperture radar (SAR) in the savannahs of north Australia

J. N. COLLINS*†, L. B. HUTLEY†§, R. J. WILLIAMS‡§, G. BOGGS†, D. BELL¶ and R. BARTOLO+

†School of Science and Primary Industries, Charles Darwin University, Darwin, NT, 0909, Australia
‡CSIRO Sustainable Ecosystems, PMB 44 Winnellie, Northern Territory, 0821, Australia
§Cooperative Research Centre for Tropical Savanna Management, Charles Darwin University, Darwin, NT, 0909, Australia
¶GecOz Pty Ltd, Cullen Bay, NT 0800, Australia
+Environmental Research Institute of the Supervising and Scientist, Department of the Environment and Water Resources GPO Box 461, Darwin NT 0801, Australia

(*Received 2 February 2007; in final form 6 December 2007*)

This study investigates the use of polarimetric AirSAR (TopSAR) data for estimating biomass and carbon storage of *Eucalyptus miniata* (Darwin Woolly Butt) and *E. tetrodonta* (Stringybark) dominated open-forest savannah in the Northern Territory, Australia. Radar backscatter intensity was correlated with basal area for 30 plots within the Wildman River Reserve, Northern Territory. Published allometric relationships were used to convert tree basal area to estimates of above-ground biomass for each of the measured plots. Below-ground biomass was also estimated for these plots, using additional published allometric relationships between below-ground and above-ground biomass. Backscatter of the L-HV channel had the highest regression co-efficient (r^2=0.92) with ground-based tree basal area measurements. Using a linear regression equation of backscatter intensity for the L-HV channel versus above-ground biomass gave a mean above-ground biomass of 94 t DM (dry mass) ha^{-1} for the eucalypt dominated vegetation in the Wildman River Reserve, equivalent to 47 t C ha^{-1} stored in this biomass pool. Estimated below-ground biomass was 28 t C ha^{-1}, giving a total carbon biomass storage for this savannah ecosystem of 75 t C ha^{-1}. The results of this study indicate that the L-HV channel of polarimetric SAR is best suited to model biomass of the tropical savannahs of northern Australia. Given the vast spatial extent of savannah woodlands across north Australia, SAR has the potential to be a major tool in carbon stock assessment, critical for carbon accounting, as well as to contribute to gaining a better understanding of the role the tropical savannahs of northern Australia play in the biochemical cycles of Australia.

1. Introduction

Savannahs are a substantial biome globally and contain approximately 58.7 Pg of biomass and account for approximately 40% of the global carbon store (House and

*Corresponding author. Email: james.collins@nrw.qld.gov.au

International Journal of Remote Sensing
ISSN 0143-1161 print/ISSN 1366-5901 online © 2009 Taylor & Francis
http://www.tandf.co.uk/journals
DOI: 10.1080/01431160802448935

Hall 2001). They therefore have the potential to significantly influence the global carbon cycle (Chen *et al.* 2003). Tropical savannahs are an extensive ecosystem of northern Australia, occupying an area of approximately 2 million km^2, approximately 25% of the Australian continental land area, and are an important ecosystem in terms of Australia's continental carbon balance (Williams *et al.* 2004). In fact this area represents 12% of the world's savannah biome and is considered to have some of the most extensive and intact *Eucalyptus* open-forest systems given the low population density (Woinarski *et al.* 2007). The composition and structure of these savannahs is largely determined by soil water availability, plant available nutrients and fire frequency (Williams *et al.* 1997). There is detailed ecological and plant physiological literature describing the northern tropical savannahs of Australia; biomass distribution and carbon balance (Burrows *et al.* 2002, Chen 2002, Chen *et al.* 2003, Beringer *et al.* 2007), ecophysiology (Eamus and Prior 2001), below-ground biomass (BGB) (Eamus *et al.* 2002), water use (O'Grady *et al.* 1999), fire regimes (Williams *et al.* 2002), leaf area index (LAI) and standing biomass (O'Grady *et al.* 2000). Although there is abundant literature on the remote sensing of fire in the savannahs of northern Australia (Russell-Smith *et al.* 2003), few studies have focused on the characteristics of forest structure, with most studies focusing on broad land cover classification of the extensive floodplain *Melaleuca* communities (Menges 2000, Bartolo 2005) or the *Eucalyptus* dominated woodland/open forest savannah (Lucas *et al.* 2000, 2002, Khwaja *et al.* 2003).

A fundamental tool in carbon accounting is tree-based allometry, whereby easily measured variables can be used to estimate above-ground biomass (AGB). O'Grady *et al.* (2000) calculated allometric relationships using power functions ($y=ax^b$) for the six most abundant tree species (*Eucalyptus tetrodonta, E. miniata, Erythrophyleum chlorostachys, Terminalia ferdinandiana, E. porrecta* and *E. bleeseri*) of the *E. tetrodonta*/*E. miniata* mesic savannahs of northern Australia. This study found that for individual trees there was a highly significant relationship between diameter at breast height (DBH; 1.30 m above the ground surface) and AGB. More importantly a single community relationship that accounted for the six dominating species was found, suggesting reliable estimates of AGB for *Eucalyptus* dominated communities in Northern Australia can be obtained with a generic relationship. Williams *et al.* (2005) corroborated this for a larger sample of species from 14 different woodland species, mainly eucalypts, from 11 sites across the Northern Territory, Queensland and New South Wales. Again, a generic equation relating tree DBH with biomass provided a high precision estimates of AGB.

The Kyoto Protocol has brought about heightened interest in terrestrial carbon dynamics, although there remains large uncertainty relating to terrestrial carbon stocks and flows, especially in tropical ecosystems such as savannah. The extent to which intact or low disturbance forests are currently acting as sinks for atmospheric CO_2 is not clear (Malhi *et al.* 1999). To fully understand the role the savannahs of northern Australia play in the continental carbon cycle, complete carbon inventories of forest stands need to be coupled with good estimates of carbon fluxes and the impact of fire (Beringer *et al.* 2007).

Tools that will enable carbon stock estimates in the savannahs at landscape and regional scales are needed. Remote sensing of terrestrial ecosystems has been recognized as a tool that can obtain data that enables both inventory and process studies to be undertaken at landscape scales (Harrell *et al.*1997, Kasischke *et al.* 1997, Leckie and Ranson 1998). Remote sensing of forested ecosystems has primarily involved analysis in the spectral domain (Lefsky *et al.* 1997) focusing on using data from systems operating in the visible and near-infrared (NIR) regions of the electromagnetic spectrum. However, within the tropical regions, wet season cloud and smoke haze during the dry season limit the use of optical sensors (Stibig *et al.* 2003) and makes seasonal monitoring impractical. In addition visible to infrared (IR) sensors are unable to detect stand characteristics that can be directly correlated to biomass (Harrell *et al.* 1997) and these features of optical sensors limit their utility in tropical regions.

Alternately, imaging radar (radio detection and ranging) is increasingly used as a method of estimating forest structure. Backscatter intensity of polarimetric synthetic aperture radar (SAR) can be correlated with DBH/basal area, making it an ideal correlate for AGB. SAR has a number of advantages over optical sensors: (1) it has the capacity to penetrate cloud, rain and smoke haze, common in the wet/dry tropical savannahs regions; (2) SAR is an active sensor with a controlled power outlet, ensuring consistent transmit/return rates independent of solar radiation variations which affect spectral reflectance measurements from optical/IR sensors; and (3) SAR can penetrate forest canopies to gather information on the forest structure as a function of the varying backscatter mechanisms experienced by the different transmitted microwave frequencies (Kasischke *et al.* 1997). There is great potential to combine remote sensing technology, in particular radar data, with existing allometric relationships (e.g. O'Grady *et al.* 1999, Williams *et al.* 2005) to map above- ground and below-ground woody biomass and obtain vegetation carbon stock estimates at landscape scales with a high degree of precision. If such tools could be developed, regular monitoring using this methodology could provide information on decadal patterns of carbon accumulation or loss from ecosystems.

This paper examines the relationship between the AGB of a northern Australian *Eucalyptus* open-forest and woodland savannah and backscatter intensity of polarimetric SAR data. This relationship and other published relationships are used to map AGB, BGB and carbon storage at a landscape scale for an extensive savannah type of north Australia.

2. Methods

2.1 *Study area*

The study area covers the Wildman River Reserve (WRR) in the Mary River region of the Northern Territory, Australia. This area is located approximately 100 km east of Darwin (figure 1) and is representative of the mesic savannahs of northern Australia (>1200 mm annual rainfall), regionally important savannah communities dominated by *Eucalyptus tetrodonta* and *E. miniata*, occupying an area of approximately 135 000 km^2 across the Northern Territory (Fox *et al.* 2001). *E. tetrodonta* and *E. miniata* account for greater than 70% of the overstorey leaf area index and standing biomass (O'Grady *et al.* 1999). This vegetation forms an open overstorey canopy with less than 50% cover with a variety of annual and perennial C4 grasses (e.g. *Sorghum spp.*) dominating the understorey (Day *et al.* 1979, Wilson *et al.* 1990, Lynch 1996, Williams *et al.* 1997, Fox *et al.* 2001). Canopy height ranges from 14 to 25 m depending on soil type and depth. Also contributing to forest biomass of the upper stratum is *Erythrophleum chlorostachys*.

The climate of the WRR region is wet-dry tropical, and is influenced by the north-west monsoon (Wilson *et al.* 1990) which results in two distinct seasons. The wet

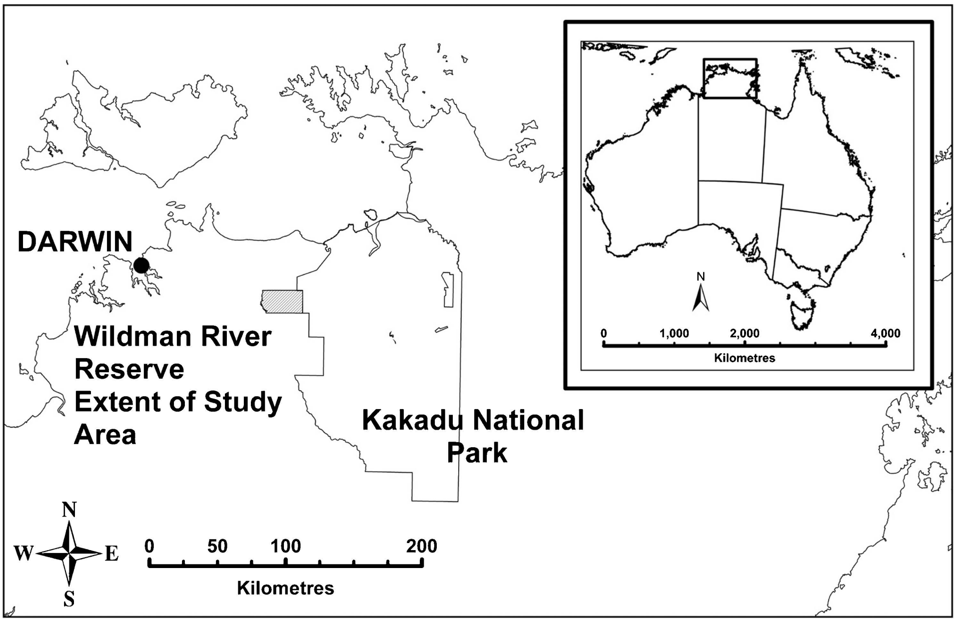

Figure 1. Location of study area.

season features high rainfalls with 90% of the annual rainfall of 1300 mm falling between November and March, often associated with cyclonic activity (Napier and Steen 2002). The 10th and 90th percentiles of annual rainfall at this site are ~1000 mm and 1800 mm, respectively (Tunstall *et al.* 1998). The dry season lasts from May to September, is virtually rainless and is characterized by south-easterly trade winds (Wilson *et al.* 1990, Napier and Steen 2002).

2.2 *Imagery*

The Airborne Imaging Radar Synthetic Aperture Radar (AirSAR) data used in this study were acquired at the end of the dry season (September) 2000 by the NASA Jet Propulsion Laboratories (JPL) during the Pacific Rim (PACRIM) 2000 campaign (Menges *et al.* 2002). Two adjacent strips of AirSAR data were acquired in TopSAR mode of the study area. Each strip was approximately 10×60 km and covered the Mary River floodplain and its surrounding savannah vegetation. The AirSAR system collects all four polarizations HH (horizontal transmit and receive), HV (horizontal transmit and vertical receive), VH (vertical transmit and horizontal receive (the same as HV)) and VV (vertical transmit and receive) for two frequencies: L-band ($\lambda \sim 24$ cm), and P-band ($\lambda \sim 68$ cm), while operating as an interferometer at C-band ($\lambda \sim 6$ cm) to simultaneously generate topographic height data (Bartolo *et al.* 2002). C-band was not utilized in this study as it is unable to penetrate canopies, interacting only with the leaves and small and secondary branches (Leckie and Ranson 1998).

The NASA/JPL AirSAR range direction, perpendicular to the flight path, has an incidence angle that typically ranges from 20° to 60°. This variation in incidence angle affects the backscatter characteristics of the land cover (Menges *et al.* 2001a). To correct for the effect of incidence angle on backscatter characteristics, a methodology developed by Menges *et al.* (2001a, 2001b) was applied to the data. The correction is based on a histogram matching process between lines of constant angle.

The TopSAR data were each registered to a 1 : 50 000 topographic map using 20 ground control points for each strip of imagery with a root mean square error (RMSE) of <1 pixel error and resampled to a $10\,\text{m} \times 10\,\text{m}$ resolution (Menges *et al.* 2001b). A mosaic of the two datasets was then produced to make one full scene of the Mary River catchment and its surrounds.

To allow more accurate and faster processing, the imagery was overlaid with Land Recourses of the Wildman River Station 1 : 50 000 data (Day *et al.* 1979) to identify targeted vegetation types and to mask unwanted areas including floodplain vegetation, *Melaleuca* forest and grasslands. The resulting data were six bands of imagery in the L and P-bands with the HH, VV and HV polarizations for the savannah vegetation of the Mary River catchment.

2.3 *Field plot selection*

A total of eight sites within the image area were selected that represented a range of standing biomass and a GPS (Global Positioning System) location was taken at each site.

A local spatial statistic developed by Menges *et al.* (2002) and applied to biomass estimation by Bartolo (2005) was used to derive an optimal field sampling size for every pixel within the image to minimize the effect of registration error and to account for heterogeneity. The statistic is based on the average digital number (DN) values within a window of increasing dimensions and assesses the variation occurring through a positional error. It is calculated by moving an image window through neighbouring locations and determining the standard deviation of the respective mean values Menges *et al.* (2002). Figure 2 outlines the application of the statistic to a single point in the image.

The statistic provides a measure of homogeneity and highlights spatially where the local variance is less than the global average. The implementation of the spatial statistic when undertaking quantitative remote sensing applications facilitates and improves the field sampling efficacy and efficiency (Menges *et al.* 2002).

The spatial statistic was applied to the six bands of imagery to determine the optimal location and size for field plots. The images produced had DN ranging from 0–15 depending on the dominant scale of spatial patterns within the image. The suggested field plot sizes ranged from $30 \times 30\,\text{m}$ to $>310 \times 310\,\text{m}$ depending on the DN. The images were density sliced to give a colour scale on the optimal field plot size for each location on the image for easy identification.

For each site, the spatial statistic was used to determine the minimum field plot size required to capture variability within the image for each location. Across the eight sites 30 study plots were determined in this manner that represented the range of biomass found within the WRR. Plot sizes were either $30 \times 30\,\text{m}$ or $50 \times 50\,\text{m}$.

2.4 *Biomass estimation*

Plot estimates of AGB were derived from measured DBH using the allometric relationships (power functions) as described by Williams *et al.* (2005). Multi-stemmed or forked trees were measured separately as each pole interacts with the radar signal and affects the returned backscatter. These allometric regression

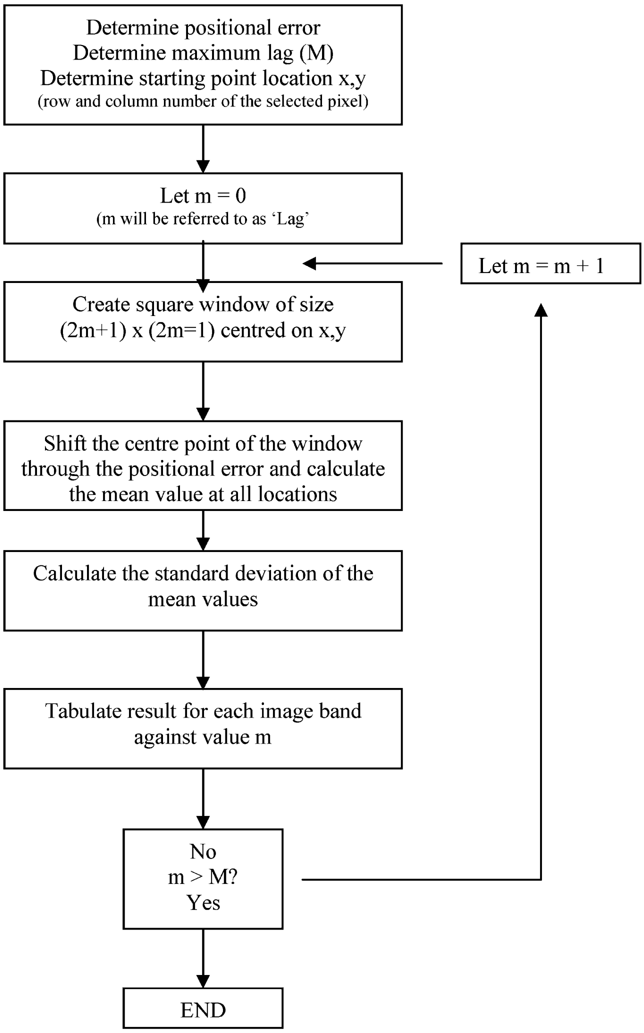

Figure 2. Procedure for applying the statistic to a single point in the image (Menges *et al* 2002).

equations were derived from 14 different woodland species, mainly Eucalypts, from 11 sites across the Northern Territory, Queensland and New South Wales. Williams *et al.* (2005) found there was a strong correlation ($r^2=0.95$) between DBH and AGB. This study found that a single, generic, species-independent relationship could be applied to all trees with little loss or no loss in precision (Williams *et al.* 2005). This equation is readily applicable to all woody species within the WRR image and is given as:

$$\mathrm{AGB} = -2.3046 + 2.5243\ln(D), \tag{1}$$

where AGB is above-ground biomass (kg) and D is DBH (cm) (equation 5(b), Williams *et al.* 2005).

Below-ground biomass (BGB) was estimated using relationship given by Eamus *et al.* (2002) who derived relationships between AGB and BGB for a number of common savannah tree species of the Darwin and WRR regional, given as:

$$\mathrm{BGB} = 26.99 \ln(\mathrm{AGB}) - 57.024, \quad (2)$$

where BGB and AGB are in kg (Eamus *et al.* 2002). The carbon fraction of woody components of vegetation above- and below-ground was assumed to be 0.49 of dry weight (Gifford 2000a, 2000b) and using this fraction, total carbon storage for each plot was calculated for both the above-and below-ground carbon pools in $\mathrm{t\,C\,ha^{-1}}$.

2.5 *Model fitting*

Backscatter intensities for P and L-bands and all polarization combinations were extracted from the WRR image using an IDL program developed in ENVI 4.0 (ENVI 2003). AGB and structural components (basal area and stem density) data for the 30 field plots were then randomly separated into two groups: (i) 15 calibration plots were used to develop a radar based regression model for estimating AGB from a relationship between DBH/basal area and backscatter; and (ii) 15 verification plots to independently test regression models developed using the calibration plots (after Harrell *et al.* 1997). The relationship between backscatter intensity (response variable) and AGB (predicted variable) was analysed using simple linear regression. Separate regressions were developed for the backscatter intensities of all polarization combinations for both L and P-bands and ANOVA and the r^2 values of the regressions were used to determine models for biomass estimation. The model with the highest regression coefficient was then used to predict the AGB of the 15 remaining test plots as a model validation exercise. In this case, backscatter was the predictor variable and AGB was the response variable. The predicted values were then regressed against the actual field estimates of AGB and used to quantify the accuracy of the model in terms of r^2, slope and y-intercept parameters. The AGB-backscatter regression model was then applied to the 22 280 ha of eucalypt dominated savannah within the WRR imagery and AGB mapped based on the spatial variation in backscatter intensity. Maps of BGB were then derived from AGB using equation (2) and carbon storage maps for woody components of the *Eucalyptus* dominated savannah were produced for the WRR as a whole.

Structural components (basal area and stem density) of the calibration plots were also analysed as a function of the varying backscatter to determine the effectiveness of SAR as a tool for estimating forest structural features in *Eucalyptus* dominated savannah. ANOVA and the r^2 values of the regressions were used to determine whether a relationship existed and which channel was best suited.

3. Results

3.1 *Model development*

Plots were representative of the open-forest and woodland savannahs, variously dominated by *Eucalyptus spp*. on red soils and shrublands dominated by *Grevillea* and *Melaleuca* on grey soils. Biomass and structural data for both calibration and verification plots are given in table 1. For the calibration plots, basal area ranged between 2.1 and $20.1\,\mathrm{m^2\,ha^{-1}}$ with the 10th and 90th percentiles being $3.6\,\mathrm{m^2\,ha^{-1}}$ and $14.9\,\mathrm{m^2\,ha^{-1}}$ respectively. Above-ground biomass ranged from 11.0 t DM (dry mass) $\mathrm{ha^{-1}}$ to $171.2\,\mathrm{t\,DM\,ha^{-1}}$ with the 10th and 90th percentiles being $19.4\,\mathrm{t\,DM\,ha^{-1}}$ and $125.3\,\mathrm{t\,DM\,ha^{-1}}$ respectively. Stem density ranged from 124

Table 1. Structural characteristics of the 30 biomass plots used within the WRR image. Calibration plots (15) were used to develop backscatter-AGB regression models with results compared to AGB estimates of the 15 verification plots. Vegetation consisted of *Eucalyptus tetrodonta*, *E. miniata* and *Erythrophyleum chlorostachys* dominated open-forest (~50% cover) or woodland (20–50% cover) savannah. Soils were red or grey kandsols (after Isbell 1996). Plots marked with * were seasonally inundated and had a reduced canopy height and were floristically distinct with *Grevillia spp., Melaleuca spp. and Calitrix spp*. significant. All plots were 30 × 30 m except those marked with † which were 50 × 50 m plots.

Model calibration plots				Model verification plots			
Plot no.	Biomass ($t\,ha^{-1}$)	Basal area ($m^2\,ha^{-1}$)	Stems (ha^{-1})	Plot no.	Biomass ($t\,ha^{-1}$)	Basal area ($m^2\,ha^{-1}$)	Stems (ha^{-1})
1	29.94	5.4	451	4	122.7	14.6	242
2	50.52	8.4	165	7†	28.8	4.4	260
3†	125.60	14.6	276	8†	72.9	6.5	220
5	171.18	20.2	297	10†	106.2	13.1	284
6*†	36.10	4.8	124	13	49.2	7.1	209
9*	11.03	2.1	572	14	107.1	14.2	572
11	55.67	7.8	385	15†	91.6	11.2	212
12	121.45	14.5	440	19	40.8	5.9	396
16†	35.71	4.6	236	23*	9.9	3.1	572
17	50.24	7.2	462	25	131.5	15.0	165
18	60.87	8.7	374	26	118.8	15.5	363
20	88.65	11.5	396	27	113.6	13.8	286
21	64.51	10.6	297	28	174.4	20.1	264
22*	12.31	3.0	979	29	118.2	14.5	198
24	124.95	15.1	220	30	47.1	6.4	187

stems ha^{-1} to 979 stems ha^{-1} with the 10th and 90th percentiles being 187.0 stems ha^{-1} and 528.0 stems ha^{-1} respectively. Structural data for the verification plots fell within these ranges. AGB was highest on well drained red-soils and lowest for shrubland vegetation which was seasonally inundated grey sandy loams.

Regression analysis for AGB (predictor variable) versus backscatter (response variable) for the L and P-bands from calibration plots are given in table 2. Scatter plots for these datasets are given in figures 3(*a*)–3(*f*). The regression statistics indicate that all channels are significant at the 95% confidence interval except the P-VV channel. The L-HV channel showed the strongest relationship between backscatter and tree biomass with an r^2 of 0.92 (table 2) and this model was chosen for predicting AGB:

$$bs = 0.00007\mathrm{AGB} + 0.0018, \tag{3}$$

where *bs* is radar backscatter intensity and AGB is in $t\,DM\,ha^{-1}$. Equation (3) was then inverted to form the model that would predict AGB from the L-HV band *bs* (figure 4) for the remaining 15 verification plots:

$$\mathrm{AGB} = 13512\, bs - 18.698 \tag{4}$$

Regression analysis for basal area and stem density (predictor variable) versus backscatter (response variable) for the L and P-bands from calibration plots are given in tables 3 and 4 respectively. Similarly the regression statistics for basal area versus backscatter indicate that all channels are significant at the 95% confidence interval except the P-VV channel. The L-HV channel, like the biomass and

Table 2. Regression analyses for the 15 calibration plots, relating AGB to backscatter intensity (*bs*) for L and P-band, with various polarizations. All channels are significant at the 95% confidence interval except the P-VV channel. The equation in bold indicates the frequency and polarization combination that represented the highest correlation with AGB.

Frequency & polarization	Regression equation	R^2	F (1,13) value	*P* value
L-HH	AGB=0.0002*bs*+0.00234	0.449	10.57	$P<0.05$
L-VV	AGB=0.0002*bs*+0.011	0.586	18.43	$P<0.05$
L-HV	**AGB=0.00007*bs*+0.0018**	**0.925**	**160.70**	$\boldsymbol{P<0.05}$
P-HH	AGB=0.0005*bs*+0.0276	0.489	12.44	$P<0.05$
P-VV	AGB=0.0001*bs*+0.0198	0.089	1.27	$P>0.05$
P-HV	AGB=0.0000*bs*+0.0035	0.296	5.50	$P<0.05$

backscatter relationship, showed the strongest relationship between basal area and backscatter with an r^2 of 0.90 (table 3). The regression statistics for stem density versus backscatter indicate that all channels are not significant at the 95% confidence interval and all channels had a very poor relationship with all r^2 values below 0.2 (table 4).

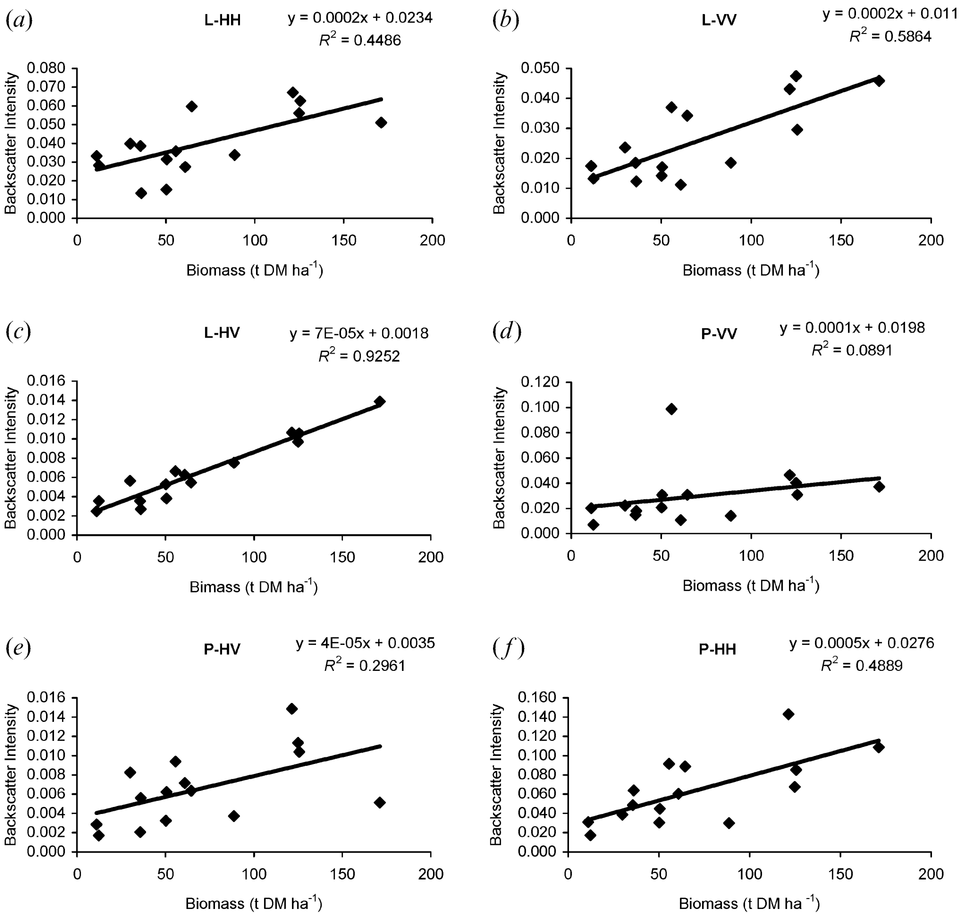

Figure 3. Plots of backscatter intensity versus biomass (t DM ha^{-1}) for various polarisations (VV, HH, HV) of both L and P-bands.

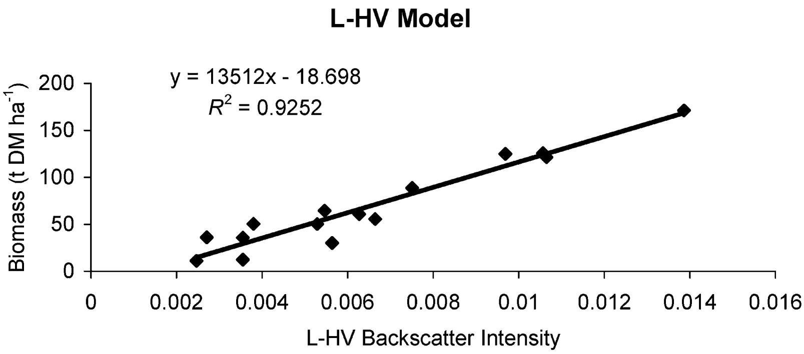

Figure 4. Scatter plot of biomass verses L-HV radar backscatter intensity, the regression model with the highest correlation.

3.2 *Biomass model verification*

The regression relationship between L-HV *bs* and AGB was tested by comparing observed and predicted AGB for the 15 verification plots. The mean observed AGB for the verification plots was 90.5 t DM ha^{-1} (sd 46.2) with the predicted AGB having a mean of 84.6 t DM ha^{-1} (sd 41.1). These means were not significantly different and the slope of observed and predicated AGB (figure 5) was not significantly different to 1 (slope=0.81 ± 0.11) with an offset (12.9 ± 11.1), also not significantly different from zero.

3.3 *Vegetation carbon pool maps*

The vegetation carbon pool for the WRR site was mapped using the regression models of AGB and BGB. AGB and BGB images were generated from the models and added together and then multiplied by the carbon mass fraction (0.49) in ENVI band math (ENVI 2003) to produce one image representing carbon storage for the eucalypt dominated vegetation in WRR (figure 6). Mean AGB for the WRR image was 94 t DM ha^{-1} (sd 57.3, range 2.9–770), with a mean BGB of 60 t DM ha^{-1} (sd 24.0, range 15.4–339). This gave a total vegetation carbon pool of 75 t C ha^{-1} for the image (table 5). For comparison, mean values of AGB, BGB and total C for the 30 measured plots were 79.1 (sd 46.6, range 11.4–178.1), 51.5 (sd 22.2, range 6.5–83) and 65.5 t C ha^{-1} (table 5). The range of biomass from the image with the highest

Table 3. Regression analyses for the 15 calibration plots, relating basal area (m^2 ha^{-1}) to backscatter intensity (*bs*) for L and P-band, with various polarizations. All channels are significant at the 95% confidence interval except the P-VV channel. The equation in bold indicates the frequency and polarization combination that represented the highest correlation with basal area.

Frequency & polarization	Regression equation	R^2	F (1,13) value	P value
L-HH	$y=0.0022x+0.0194$	0.464	11.27	$P<0.05$
L-VV	$y=0.0019x+0.0077$	0.594	19.03	$P<0.05$
L-HV	$y=0.0006x+0.0008$	0.900	**116.99**	$\boldsymbol{P<0.05}$
P-HH	$y=0.0047x+0.02$	0.483	12.14	$P<0.05$
P-VV	$y=0.0013x+0.0173$	0.094	1.35	$P>0.05$
P-HV	$y=0.0004x+0.0029$	0.299	5.53	$P<0.05$

Table 4. Regression analyses for the 15 calibration plots, relating stem density (ha^{-1}) to backscatter intensity (*bs*) for L and P-band, with various polarizations. All channels were not significant at the 95% confidence interval.

Frequency & polarization	Regression equation	R^2	F (1,13) value	P value
L-HH	$y=-1E\text{-}05x+0.0443$	0.025	0.33	$P>0.05$
L-VV	$y=-2E\text{-}05x+0.0313$	0.059	0.81	$P>0.05$
L-HV	$y=-3E\text{-}06x+0.0077$	0.039	0.53	$P>0.05$
P-HH	$y=-6E\text{-}05x+0.0866$	0.134	2.01	$P>0.05$
P-VV	$y=-6E\text{-}06x+0.0087$	0.097	0.56	$P>0.05$
P-HV	$y=-1E\text{-}05x+0.0443$	0.025	1.40	$P>0.05$

range ($>200\,t\,C\,ha^{-1}$) accounted for only 1.2% of the pixels within the carbon image and 29% of the total carbon fell in the range 50–75 $t\,C\,ha^{-1}$ (figure 7).

4. Discussion

This study clearly demonstrated the potential of SAR for predicting and mapping biomass and thus carbon stocks at landscape scales in the tropical savannahs of northern Australia. The L-band, particularly the L-HV channel, was found to have the highest correlation between backscatter and AGB ($r^2=0.92$), enabling relatively precise estimations for the *Eucalyptus* dominated open forest savannahs in the WRR. Although the L-HV channel in this study showed the strongest relationship, the L-band (all polarizations) and the P-HH and P-HV relationship were all significant as well. This result is similar with the results reported by Lucas *et al.* (2000, 2002) for a Queensland woodland. Lucas *et al.* (2000) found JERS-I SAR L-HH and AirSAR P-HV and P-HH had the strongest relationships with AGB. Lucas *et al.* (2002) found the L-band AirSAR had a strong relationship with AGB although it was found that the L-VV had the highest correlation with AGB.

The highest value of AGB estimated from plot measurements in the field was $174\,t\,DM\,ha^{-1}$, yet the highest mapped result was $770\,t\,DM\,ha^{-1}$, a clear anomaly, as reported biomass for dense tropical rainforests stands are below 400–$500\,t\,DM\,ha^{-1}$ (Mahli *et al.* 1999). These anomalies (with some values exceeding $200\,t\,DM\,ha^{-1}$) accounted for less than 5.5% of pixels within *Eucalyptus* dominated

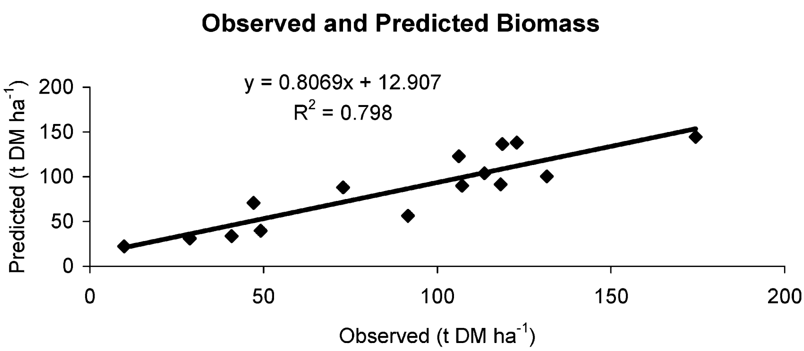

Figure 5. Observed and predicted biomass for the 15 verification plots. Predicted values were calculated from equation (4) and the observed values from combined community equation (1).

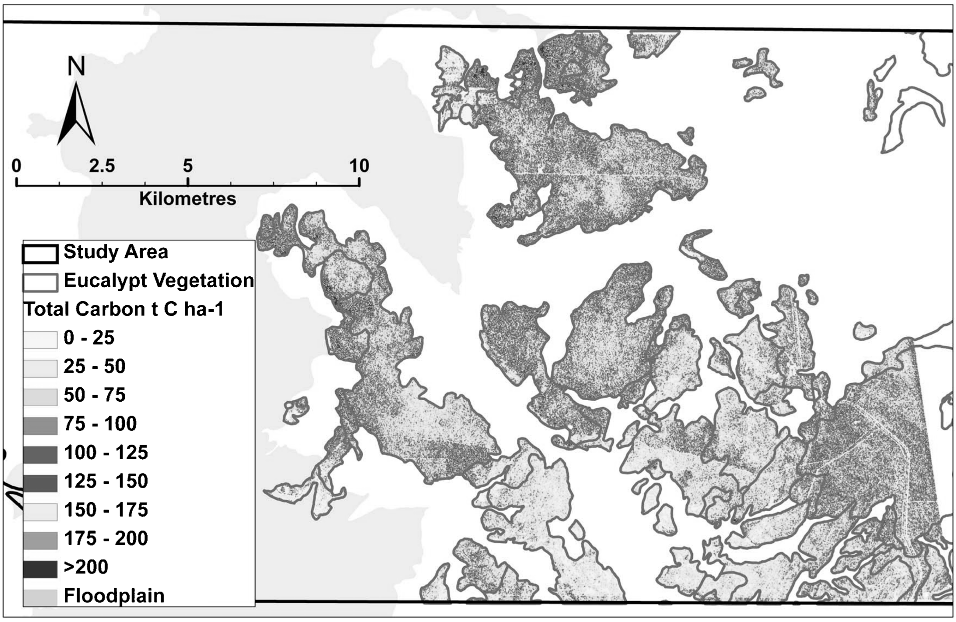

Figure 6. Map of the estimated total carbon storage within the eucalypt dominated vegetation of the WRR.

Table 5. Comparison of this studies biomass estimates and other studies undertaken in vegetation broadly similar to tropical savannahs.

Vegetation type	AGB t DM ha^{-1} (sd)	BGB t DM ha^{-1} (sd)	Total t C ha^{-1} (sd)	Source
Eucalypt savannah open-forest WRR radar image	94 (57.3)	60 (24.0)	75 (40.2)	This study
Eucalypt savannah open-forest plot data	79.1 (46.6)	51.5 (22.2)	65.5 (32.7)	This study
Eucalypt savannah open-forest	55			O'Grady et al. (2000)
Eucalypt savannah open-forest	67.2 (15.4)	38.4 (25.2)	53 (20)	Eamus *et al.* (2002), Chen *et al.* (2003)
Queensland Woodland near Injune	71.5 (29.9)			Lucas *et al.* (2000)
Queensland Woodland near Talwood	57			Lucas *et al.* (2000)
Woodlands and scrublands	20–150			Whittaker and Woodwell (1971)
Sub-tropical eucalypt open-forest	100			Westman and Rogers (1977)
Global mean—topical savannahs			20–150	Teissen *et al.* (1998)
Global mean—tropical savannah	21.6 (18.4)	40 (30.8)	33.0 (22.9)	Grace *et al.* 2006
Global mean—tropical dry forests			75	Scholes and Hall (1996)
Global mean—savannah woodland	62 (28)			Scholes and Hall (1996)

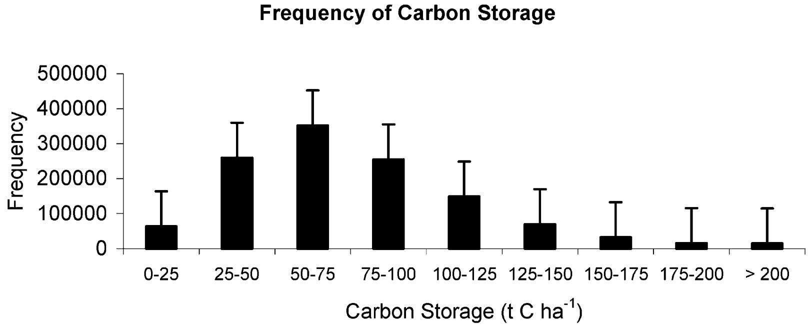

Figure 7. Frequency histogram of the estimated total carbon storage within the eucalypt dominated vegetation of the WRR.

vegetation of the WRR, however ground-truthing revealed that these pixels were clearly associated with riparian zones and uneven terrain. When applying this model at the landscape scale it is likely that such anomalies will occur and this highlights the need to identify and remove these values from a final dataset. Given the relative ease of identification of these outliers, and the statistically significant performance of the model compared to an independent validation dataset, the model was found to be robust and appropriate for application at the landscape scale.

Overall, this study produced higher biomass estimates when compared to other open-forest savannah sites near Darwin (O'Grady *et al.* 1999, Eamus *et al.* 2002, Chen *et al.* 2003, table 5). Mean AGB for the *Eucalyptus*-dominated savannah within the WRR was 94 t DM ha^{-1}, compared to only 55 t DM ha^{-1} as given by O'Grady *et al.* (1999). Similarly, mean BGB for WRR is 60 t DM ha^{-1} compared to 38.4 t DM ha^{-1} for the Darwin sites used by Eamus *et al.* (2002). However these differences are likely to reflect stand structure of the two regions, rather than a systematic over-estimation of biomass by the radar-based method. There are three likely reasons for these differences. Firstly, the study of O'Grady *et al.* (1999) was conducted on the Gunn Point peninsula near Darwin, a region that may still be recovering from the impact of Cyclone Tracy (1974) which resulted in extensive tree damage; current size class distribution reflects a young, recovering open-forest that may not have reached maturity (Bowman 1986, O'Grady *et al.* 2000). This cyclone did not affect the WRR site. Secondly, fire is a major influence on the structure and biomass of savannahs and frequent fire is likely to reduce biomass accumulation in these savannahs (Williams *et al.* 2004). The Darwin sites (crown land) are subjected to near annual burning with little or no management when compared to fire management and practices of the WRR, an environmental reserve with active fire management provided by government park authorities. Thirdly, soil structure and depth differ between the sites. Although soils of both sites are red or grey kandsols and part of the Koolpinyah surface (an extensive sand sheet of coastal Northern Territory), the soils of the WRR plots have a deeper profile (~3–5 m) with lower gravel content (personal observation) and thus superior water and nutrient holding capacity (Day *et al.* 1979) when compared to the gravely nature (20–50% by volume) of red kandsols soils of the Darwin sites. The dominant trees at the WRR were up to 25 m tall and represent a well developed *E. tetrodonta* and *E. miniata* open-forest savannah type and the observed differences in AGB between these studies represents typical spatial variability.

AGB and total vegetation carbon estimated here are also higher than published global means for savannahs, reflecting the significant woody component of these mesic savannahs. Values of vegetation carbon pool given here are identical to global means for tropical dry forest and woodlands given by Scholes and Hall (1996) and are within the range given for savannah of Teissen *et al.* (1998) (table 5). Estimates from this study are also comparable to *Eucalyptus* open-forests and woodlands of in sub-tropical and temperate Australia, which have an estimated standing biomass of approximately 100 t DM ha^{-1} (Westman and Rogers 1977), 71.5 t DM ha^{-1} and 57 t DM ha^{-1} mixed *Acacia*, *Eucalyptus* and *Callitris* woodland near Injune and Talwood Queensland respectively (Lucas *et al.* 2000) (table 5) and well within the range of 20–150 t DM ha^{-1} reported by Whittaker and Woodwell (1971) for southern Australian woodlands and scrublands (table 5).

The method used to estimate BGB in this study used the relationship between two parameters that have both been estimated, rather than directly measured, introducing additional errors in final estimates. A more accurate way of estimating biomass is to use the method described by Komiyama *et al.* (1987). This method uses tree-to-tree distance and DBH of each to estimate the BGB. However obtaining tree-to-tree distance using SAR is difficult given the spatial scale (10 m $\times$ 10 m) of the data and the density of the woodlands and the only way of determining the accuracy of the BGB estimates is plot based field verification utilizing the above method or to excavate all trees within a range of plots, an expensive and time consuming exercise.

This study also demonstrated the potential of SAR for predicting and mapping structural components of the tropical savannahs of northern Australia. The L-HV channel was found to have the highest correlation between backscatter and basal area (r^2=0.90). This result is not surprising as DBH/basal area is closely related to biomass (O'Grady *et al.* 2000, Williams *et al.* 2005). The correlations (r^2) between backscatter and basal area found in this study are higher than those reported by Harrell *et al.* (1997)—L-HV r^2=0.79 and r^2=0.69 for a pine forest in south-eastern America (SIR-C data)—and Beaudion *et al.* (1994)—L-HV r^2=0.76 pine forest (SAR data). No relationship between backscatter and stem density was found in this study. Beaudion *et al.* (1994) reported similar results for a pine forest using SAR data. All r^2 reported in this study were below 0.2.

No saturation of the L-HV channel was observed in this study for biomass levels of up to 174 t DM ha^{-1}. This finding is not consistent with Hoekman and Quinones (1998) who reported saturation of the L-band at 40–60 t ha^{-1}, Imhoff (1995) who reported saturation in the P and L-bands at 100 t ha^{-1} and 40 t ha^{-1}, respectively, and Dobson *et al.* (1992), who reported saturation at levels 100 t ha^{-1} for L-band. These saturation levels are considerably lower than the biomass levels estimated in this study, which were more consistent with the P-band saturation levels found by Hoekman and Quinones (1998), i.e. 100–300 t ha^{-1}, and Dobson *et al.* (1992), i.e. 200 t ha^{-1}.

The strengths of the relationships and saturation levels between biomass and backscatter are dependent on the forest being analysed (Green 1998). Saturation in certain circumstances can be a result of a reduction in the net backscatter due to the extinction of the signal within dense forest structures (Pierce *et al.* 2001). The general consensus of the literature indicates the cross polarized returns have the greatest sensitivity to variation in AGB (Dobson *et al.* 1992, Baker *et al.* 1994, Beaudoin *et al.* 1994, Rauste *et al.* 1994, Wang *et al.* 1995, Harrell *et al.* 1997). The single polarizations (HH, VV) saturate at a lower biomass level then the cross polarized returns.

In the *Eucalyptus* dominated open-forest savannahs, where canopy cover averages between 30% and 50% and basal area is low, the amount of backscatter absorbed will be minimal compared to that of higher density tropical and pine forests and would explain why no saturation of the L-HV channel was observed in this study.

4.1 *Radar based monitoring systems*

Radar remote sensing has proven to be a valuable tool for providing information on forest structure and biomass measurements over varying forested systems. Radar operates at low frequency wavelengths, L and P-bands and has the capability of penetrating canopies, enabling estimation of biomass and forest structure. This study highlights, through the strong relationships between basal area, biomass and backscatter in both the P and L-bands, the potential use for using SAR as a tool to estimate biomass and thus carbon stocks. This is significant given the growing interest in carbon storage in terrestrial ecosystems and also carbon trading options where accurate landscape scale estimate of carbon pools will be required. The water content of the dominant evergreen species, which comprise 80% of the vegetation found in the mesic savannahs of northern Australia (Williams *et al.* 1997) remains relatively constant between seasons, even though atmospheric and soil water content changes dramatically from wet to dry seasons (Hutley *et al.* 2000). Tree transpiration is aseasonal (Hutley *et al.* 2000) and water content of the tree stems will also remain relatively constant in the wet to dry season. This is an important factor, as the dielectric constant that is governed by the water content, determines the amount of radar reflection (Leckie and Ranson 1998). This will potentially allow accurate estimation of biomass and carbon stocks using radar in both wet and dry seasons.

The limitations of the technique are evident, given the large outliers in the data. These were due to the topographic variation and the different structure of the riparian vegetation, although anomalies/errors such as these can be discarded using a threshold backscatter values or masking these areas from the assessment. Whilst open-forest savannah is the dominant vegetation, there is a wide range of community types in north Australia, from high biomass seasonal rainforests and *Melaleuca* swamp forests to low tree-density grasslands and wetlands (Wilson *et al.* 1990) and each would require model development. Bartolo (2005) has developed an independent relationship for *Melaleuca* communities and coupled with relationships developed here for the extensive tropical savannah, a significant proportion of north Australia vegetation could be sampled using radar. New satellite-based SAR platforms (as opposed to airborne as used here) provide further scope for developing monitoring tools for carbon dynamics at a landscape and regional scale.

Acknowledgements

I would like to thank the CRC for Tropical Savannahs for its financial support and Charles Darwin University for the use of equipment. I would also like to thank Parks and Wildlife Commission Northern Territory and the rangers of Wildman River Reserve for allowing me access to my study sites.

References

Baker, J.R., Mitchell, P.L., Cordey, R.A., Groom, G.B., Settle, J.J. and Stileman, M.R., 1994, Relationships between physical characteristics and polarimetric radar backscatter for Corsican pine stands in Thetford Forest, UK. *International Journal of remote sensing*, **15**, pp. 2827–2849.

BARTOLO, R.E., MENGES, C.H., PHINN, S.R. and HILL, G.J.E., 2002, An examination of a SAR sensor for quantifying Melaleuca biomass on a tropical floodplain in northern Australia. *11th Australasian Remote Sensing and Photogrammetry Conference*, 2–6 September, Brisbane, Australia, pp. 647–683.

BARTOLO, R., 2005, Remote sensing of Melaleuca biomass on tropical floodplains. PhD Thesis, Charles Darwin University, Darwin.

BEAUDOIN, A., LE TOAN, T., GOZE, S., NEZRY, A., LOPES, A., MOUGIN, E., HSU, C., CHAN, H., KONG, J. and SHIN, R., 1994, Retrieval of forest biomass from SAR data. *International Journal of Remote Sensing*, **15**, pp. 2777–2796.

BERINGER, J., HUTLEY, L.B., TAPPER, N.J. and CERNUSAK, L.A., 2007, Savanna fires and their impact on net ecosystem productivity in north Australia. *Global Change Biology*, **13**, pp. 990–1004.

BOWMAN, D.M.J.S., 1996, Stand characteristics, understorey associates and environmental correlates of *Eucalyptus tetrodonta* F. Muell. forests on Gunn Point, northern Australia. *Vegetatio*, **65**, pp. 105–113.

BURROWS, W.H., HENRY, B.K., BACK, P.V., HOFFMANN, M.B., TAIT, L.J., ANDERSON, E.R., MENKE, N., DANAHER, T., CARTER, J.O. and MCKEON, G.M., 2002, Growth and carbon stock change in Eucalypt woodlands in northeast Australia: Ecological and greenhouse sink implications. *Global Change Biology*, **8**, pp. 769–764.

CHEN, X., 2002, Carbon balance of a Eucalypt open-forest savanna of northern Australia. PhD Thesis, Northern Territory University, Darwin, Australia.

CHEN, X., HUTLEY, L.B. and EAMUS, D., 2003, Carbon balance of a tropical savanna of northern Australia. *Oecologia*, **137**, pp. 405–416.

DAY, K.J., HARRISON, C. and VAN CUYLENBURG, H.R.M., 1979, Land resources of Wildman River Station, NT. Darwin, Parks and Wildlife Commission of the Northern Territory. Technical Report. Tech Memorandum 79/6.

DOBSON, M.C., ULABY, F.T., LE TOAN, T., BEAUDOIN, A., KAISISCHKE, E.S. and CHRISTENSEN, N., 1992, Dependence of radar backscatter on coniferous forest biomass. *IEEE Transactions on Geoscience and Remote Sensing*, **30**, pp. 412–415.

EAMUS, D. and PRIOR, L.D., 2001, Ecophysiology of trees of seasonally dry tropics: Comparisons among phonologies. *Advances Ecological Research*, **32**, pp. 113–197.

EAMUS, D., CHEN, X., KELLY, G. and HUTLEY, L.B., 2002, Root biomass and root fractal analysis of an open Eucalyptus forest in a savanna of north Australia. *Australian Journal of Botany*, **50**, pp. 31–41.

ENVI, 2003, Version 4.0. The Environment for Visualizing Images (Boulder, USA: Research Systems, Inc). Available at: http://www.RSInc.com/envi (accessed 2004).

FOX, I.D., NELDNER, V.J., WILSON, G.W. and BANNINK, P.J., 2001, The vegetation of the Australian tropical savannas. (Brisbane, Queensland: Environmental Protection Agency).

GIFFORD, R.M., 2000a, Carbon contents of above-ground tissues of forest and woodland trees. National Carbon Accounting System, Technical Report No 22. Australian Greenhouse Office, Canberra.

GIFFORD, R.M., 2000b, Carbon content of woody roots. (Revision 1) National Carbon Accounting System, Technical Report No 7. Australian Greenhouse Office, Canberra.

GRACE, J., SAN, J.J., MEIR, P., MIRANDA, H.S. and MONTES, R.A., 2006, Productivity and carbon fluxes of tropical savannas. *Journal of Biogeography*, **33**, pp. 387–400.

GREEN, R.M., 1998, Relationship between polarimetric SAR backscatter and forest canopy and sub-canopy biophysical properties. *International Journal of Remote Sensing*, **19**, pp. 2395–2412.

HARRELL, P.A., KASISCHKE, E.S., BOURGEAU-CHAVEZ, L.L., HANEY, E.M. and CHRISTENSEN JR, N.L., 1997, Evaluation of approaches to estimating above ground biomass in southern pine forests using SIR-C data. *Remote Sensing of Environment*, **59**, pp. 223–233.

HOEKMAN, D.H. and QUINONES, M.J., 1998, P-band SAR for tropical forest mapping and landcover change. *Earth Observation Quarterly*, **61**, pp. 18–22.

HOUSE, J.I. and HALL, D.O., 2001, Productivity of tropical savannas and grasslands. In *Terrestrial Global Productivity*, J. Roy, B. Saugier and H.A. Mooney (Eds), pp. 336–400 (San Diego, USA: Academic Press).

HUTLEY, L.B., O'GRADY, A.P. and EAMUS, D., 2000, Evapotranspiration from Eucalypt open-forest savanna of northern Australia. *Functional Ecology*, **14**, pp. 183–194.

IMHOFF, M.L., 1995, Radar backscatter and biomass saturation: Ramifications for a global biomass inventory. *Geoscience and Remote Sensing IEEE Transactions*, **14**, pp. 511–518.

ISBELL, R., 1996, *Australian Soil Classification* (Collingwood, Australia: CSIRO Publishing).

KASISCHKE, E.S., MELACK, J.M. and DOBSON, M.C., 1997, The use of imaging radars for ecological applications. *Remote Sensing of Environment*, **59**, pp. 141–156.

KHWAJA, Z.H., AHMAD, W. and WILLIAMS, R.J., 2003, An evaluation of alternative image classification techniques for the identification and mapping of tropical savanna landscape in northern Australia. *Geocarto International*, **18**, pp. 3–44.

KOMIYAMA, A., OGINO, K., AKSORNKAOE, S. and SABHASRI, S., 1987, Root biomass of mangrove forest in southern Thailand. 1. Estimation by the trench method and the zonal structure of root biomass. *Journal of Tropical Ecology*, **3**, pp. 97–108.

LECKIE, D. and RANSON, K., 1998, Forestry Applications Using Imaging Radar. In *Principles and Applications of Imaging Radar*, 3rd edn, F.M. Henderson and A.J. Lewis (Eds) (New York: John Wiley and Sons), pp. 435–509.

LEFSKY, M.A., COHEN, W.B., ACKER, S.A., SPIES, T.A., PARKER, G.G. and HARDING, D., 1997, Lidar remote sensing of forest canopy structure and related biophysical parameters at the H. J. Andrews experimental forest, Oregon, USA. In *Natural Resources Management using Remote Sensing and GIS*, J.D. Greer (Ed.), pp. 79–91 (Washington, DC: ASPRS).

LUCAS, R.M., MILNE, A.K., CRONIN, N., WITTE, C. and DENHAM, R., 2000, The potential for Synthetic Aperture Radar (SAR) for quantifying the biomass of Australia's woodlands. *Rangeland Journal*, **22**, pp. 124–140.

LUCAS, R.M., TICKLE, P., LEE, A., AUSTIN, J., WITTE, C., JONES, J., CRONIN, N., MOGHADDAM, M. and MILNE, A.K., 2002, Use of AIRSAR (POLSAR) data for quantifying the biomass of woodlands, Queensland, Australia. In *2002 AIRSAR Earth Science and Application Workshop*, 4–6 March 2002, USA.

LYNCH, D., 1996, *Mary River Floodplain vegetation.* Northern Territory Department of Lands, Planning and Environment Resource Capability Assessment Branch.

MAHLI, G., BALDOCCHI, D.D. and JARVIS, P.G., 1999, The carbon balance of tropical, temperate and boreal forests. *Plant Cell Environment*, **22**, pp. 715–740.

MENGES, C.H., 2000, Image processing of multi-frequency polarimetric AirSAR data to characterise the vegetation communities of the tropical savannas in northern Australia. PhD Thesis, Northern Territory University, Australia.

MENGES, C.H., VAN ZYL, J.J., HILL, G.J.E. and AHMAD, W., 2001a, A procedure for the correction of the effect of variation in local incidence angle on AIRSAR data. *International Journal of Remote Sensing*, **22**, pp. 829–841.

MENGES, C., HILL, G.J.E., AHMAD, W. and VAN ZYL, J.J., 2001b, Incidence angle correction of AirSAR data to facilitate land cover classification. *Photogrammetric Engineering & Remote Sensing*, **67**, pp. 479–489.

MENGES, C.H., BARTOLO, R.E., PHINN, S. and HILL, G.J.E., 2002, A spatial statistic to determine appropriate field sampling size for linking image and field data. In *11th ARSPC Seminar*, 2–6 September 2002. Brisbane, QLD, pp. 901–911.

Napier, D.E. and Steen, C.N., 2002, Upper Mary River Catchment Resource Assessment and Design Survey. Technical Report No. 31/2002. Soil and Vegetation Assessment Unit, Natural Systems Division Department of Infrastructure, Planning and Environment, Northern Territory.

O'Grady, P.A., Eamus, D. and Hutley, L.B., 1999, Transpiration increases during the season: patterns of tree water use in eucalypt open-forests of northern Australia. *Tree Physiology*, **19**, pp. 591–597.

O'Grady, A.P.O., Chen, X., Eamus, D. and Hutley, L.B., 2000, Composition, leaf area index and standing biomass of eucalypt open forests near Darwin in the Northern Territory, Australia. *Australian Journal of Botany*, **48**, pp. 629–638.

Pierce, L.E., Dobson, M.C., Soares, J.V. and Liang, P., 2001, Above-ground biomass estimation using JERS/RADARSAT SAR composites. *Anais X SBRS workshop*, 21–26 April 2001, Foz do Iguacu, Brazil (INPE), p. 1703.

Rauste, Y., Häme, T., Pulliainen, J., Heiska, K. and Hallikainen, M., 1994, Radar-based forest biomass estimation. *International Journal of Remote Sensing*, **15**, pp. 2797–2808.

Russell-Smith, J., Whitehead, P.J., Cook, G.D. and Hoare, J.L., 2003, Response of *Eucalyptus*-dominated savanna to frequent fires: lessons from Munmarlary, 1973–1996. *Ecological Monographs*, **73**, pp. 349–375.

Scholes, R.J. and Hall, D.O., 1996, The carbon budget of tropical savannas, woodlands and grasslands. In *Global Change: effects on coniferous forests and grasslands*, A.I. Breymeyer, D.O. Hall, J.M. Melillo and G.I. Agren (Eds), pp. 69–100 (New York: John Wiley).

Stibig, H.-J., Beuchle, R. and Achard, F., 2003, Mapping of tropical forest cover of insular Southeast Asia from SPOT4-Vegetation images. *International Journal of Remote Sensing*, **24**, pp. 3651–3663.

Tiessen, H., Fellar, C., Sampaio, E.V.S.B. and Garin, P., 1998, Carbon sequestration and turnover in semiarid savannas and dry forests. *Climate Change*, **40**, pp. 105–117.

Tunstall, B., Orr, T. and Marks, A., 1998, Vegetation and soil mapping Mt Bundy training area. CSIRO land and water technical report 8/98.

Wang, Y., Davis, F.W., Melack, J.M., Kasischke, E.S. and Christensen Jr, N.L., 1995, The effects of changes in forest biomass on radar backscatter from tree canopies. *International Journal of Remote Sensing*, **16**, pp. 503–513.

Westman, W.E. and Rogers, R.W., 1977, Biomass and structure of a subtropical eucalypt forest, North Stradbroke Island. *Australian Journal Botany*, **25**, pp. 171–191.

Whittaker, R.H. and Woodwell, G.M., 1971, Measurement of net primary production of forests. In *Productivity of Forest Ecosystems. Proceedings of the Brussels Symposium 1969*, P. Duvigeneaud (Ed.), pp. 159–175 (Paris: UNESCO).

Williams, R.J., Myers, B.A., Muller, M.J., Duff, G.A. and Eamus, D., 1997, Leaf phenology of woody species in a northern Australian tropical savanna. *Ecology*, **78**, pp. 2542–2558.

Williams, R.J., Griffiths, A.D. and Allan, G.E., 2002, Fire regimes and biodiversity in the wet-dry tropical landscape of northern Australia. In *Flammable Australia: The fire regimes and biodiversity of a continent*, R.A. Bradstock, J.E. Williams and A.M. Gill (Eds), pp. 281–304 (Cambridge: Cambridge Scientific Press).

Williams, R.J., Hutley, L.B., Cook, G.D., Russell-Smith, J.R.S., Edwards, A. and Chen, X., 2004, Assessing the carbon sequestration potential of mesic savannas in the Northern Territory, Australia: approaches, uncertainties and potential impacts of fire. *Functional Plant Biology*, **31**, pp. 415–422.

Williams, R.J., Zerihun, A., Montagu, K., Hoffman, M., Hutley, L.B. and Chen, X., 2005, Allometry for estimating above-ground tree biomass in tropical and subtropical eucalypt woodlands: towards general predictive equations. *Australian Journal of Botany*, **53**, pp. 607–619.

WILSON, B.A., BROCKLEHURST, P.S., CLARK, M.J. and DICKINSON, J.J.M., 1990, Vegetation of the Northern Territory, Australia. Technical Report No. 49. Conservation Commission of the Northern Territory, Australia.

WOINARSKI, J., MACKEY, B., NIX, H. and TRAILL, B., 2007, *The Nature of Northern Australia: Its natural values, ecological processes and future prospects* (Canberra: ANU Press).